Optimum conditions for thermal fixing of volume holograms in Fe:LiNbO3

Shiuan Huei Lin, C. R. Hsieh, T. C. Hsieh* and Ken Y. Hsu
Institute of Electro-Optical Engineering
*Department of Electro-Physics
National Chiao Tung University, Hsin-Chu, Taiwan, R.O.C.

Arthur E. T. Chiou
Institute of Electrical Engineering
National Dong Hwa University, Hwa-Lien, Taiwan, R.O.C.

ABSTRACT

The kinetics of the recording, compensating, and developing processes in two typical thermal fixing procedures (L-H-L and H-L procedures) are analyzed. The optimum condition (in terms of the fixing temperature, compensation time and material parameters) for each fixing procedures are obtained under the boundary condition of short-circuit. Experimental results are shown which are in qualitative agreement with the theory in L-H-L procedure.

Keywords: Photorefractive crystal, Thermal fixing, Lithium niobate crystal, Volume hologram

1. INTRODUCTION

There is considerable current interest in the use of recording the refractive index gratings in photorefractive crystals for volume holographic storage and other types of the optical-information-processing applications. Three of the main advantages are that large crystal volume can be grown with high-optical-quality, parallel readout with an ultra-fast access time is provided, and the information can be stored, retrieved and erased by the illumination of light, in real time. However, for some applications such as information storage, pattern recognition, the non-volatile photoreafractive memories are required after recording and/or processing. For this purpose, fixing of the refractive index grating is one of the key issues.

By far, thermal processing is the most popular and effective technique for the non-volatile photorefractive memories stored in Fe:$LiNbO_3$ crystals [1-9]. In general, thermal fixing is a means of transforming a photo-induced volatile (i.e. erasable by read-out beam) electronic grating into non-volatile ionic grating (which is insensitive to optical illumination) via the following three phases: (1) the recording phase, (2) the fixing (or compensating) phase, and (3) the developing phase. In the recording phase, an electronic grating evolves in the crystal (via the photorefractive effect) in response to a non-uniform illumination of light. In the fixing (or compensating) phase, the crystal is heated to an elevated temperature (usually > 400°K) when the protons (or ions) migrate to form a complementary ionic grating. With opposite charge distributions, the electronic and ionic gratings compensate each other either partially or completely. In the developing phase, the crystal (with the compensated grating pair) is cooled to near room temperature and then illuminated with an uniform (and preferably incoherent) developing beam. Since the proton migration is negligible at near room temperature, the ionic grating is frozen and developed (or manifested) as the electronic grating is gradually erased by the uniform developing beam.

While some properties of thermal fixing have been studied [10-13], the results of those studies are useful in a general sense. Obviously, fixing efficiency strongly depends on the procedures to perform thermal fixing. In other words, the thermal fixing dynamics affect the final diffraction efficiency of the fixed grating. A proper characterization is never complete without a detail look at the dynamic properties of each procedure. Therefore, some of the questions that need to be studied are the following:

- How does the dynamics of each phase change with temperature? How does the dynamics affect thermal fixing efficiency?
- Does the boundary condition of the crystal affect the thermal fixing? Does the recording scheme affect the thermal fixing?
- What time scales are reasonable for practical thermal fixing? What is the optimal values for thermal fixing in terms of the environment conditions, including fixing temperature and compensation time?

Part of the SPIE Conference on Photorefractive Fiber and Crystal Devices: Materials, Optical Properties, and Applications V • Denver, Colorado • July 1999 SPIE Vol. 3801 • 0277-786X/99/$10.00

We seek to answer these and related questions on the basis of the theoretical analysis by taking into account of the compensation effect of ions with the electronic grating in Kukhtarev's band transport model [14]. From the analysis, we deduce the optimal environmental conditions for a crystal with a given iron-doped concentration. In particular, the influences of the compensation time and the fixing temperature for the given material parameters are presented. In addition, the experiment results are presented to verify our theoretical analysis.

2. THEORETIC ANALYSIS

The main idea for those processes is that proton migration occurs in high temperature for the neutralization of the electronic grating, which was built in either low or high temperature. This ionic grating is not affected by light illumination in low temperature, as a result the phase grating is fixed in the crystal. Thus, by taking into account of the compensation effect of ions with the electronic grating in Kukhtarev's band transport model and following the similar procedures in Kukhtarev's paper[10] (i.e. separating all parameters into dc and modulation terms and then solving the coupled material equations for the dc and modulation terms, respectively. Here, we use subscripts 0 as the dc term and 1 as the modulation terms.), the dynamics of modulation of two space charge densities, the empty electron trap density ($N_{D1}^{t}(t)$) and ion density ($n_{i1}(t)$), can be given as,

$$\frac{\partial N_{D1}^{t}(t)}{\partial t} = aN_{D1}^{t}(t) + bn_{i1}(t) + c \tag{1}$$

$$\frac{\partial n_{i1}(t)}{\partial t} = dN_{D1}^{t}(t) + en_{i1}(t) \tag{2}$$

where $$a = -\frac{\omega_e \gamma_R N_A + (sI_o + \beta)\frac{N_D}{N_A}(\omega_e + D_e K^2 + j\mu_e K E_o) + j\frac{PI_o K}{q}\gamma_R N_A}{\gamma_R N_A + \omega_e + D_e K^2 + j\mu_e K E_o} \tag{3}$$

$$b = -\frac{\omega_e \gamma_R N_A}{\gamma_R N_A + \omega_e + D_e K^2 + j\mu_e K E_o} \tag{4}$$

$$c = \frac{jK\frac{P(N_D - N_A)}{q}I_1 - s(N_D - N_A)I_1}{\gamma_R N_A + \omega_e + D_e K^2 + j\mu_e K E_o}\gamma_R N_A + s(N_D - N_A)I_1 \tag{5}$$

$$d = -\omega_i \tag{6}$$

$$e = -(\omega_i + D_i K^2 - j\mu_i K E_o) \tag{7}$$

where $\omega_e \equiv \frac{q\mu_e n_{e0}}{\varepsilon}$, electronic dielectric relaxation rate, (8)

$\omega_i \equiv \frac{q\mu_i n_{i0}}{\varepsilon}$, ionic dielectric relaxation rate. (9)

The definitions and values of all the parameters are listed on Table 1. By substituting the space charge distribution into Poisson's equation, the space-charge field in the crystal can be written as,

$$E_{sc}(t) = E_0 + E_1(t)[\exp(-jKx) + c.c.] \tag{10}$$

$$\text{where } E_1(t) = \frac{jq}{\varepsilon K}\left(N_{D1}^{t}(t) + n_{i1}(t)\right) \tag{11}$$

Note that in Eq. (10), E_0 represents the dc term of the space charge field. In order to calculate $E_{sc}(t)$, equations (1)~(2) should be solve with an appropriate boundary conditions [15]. In practice, there are two cases: with and without an externally applied field. In the first case, E_0 remains constant during the grating recording period (representing short-circuit or pre-exposed open-circuit conditions). Equations (1)~(2) can be turned into a set of linear differential equations with constant coefficients. Under this situation, an analytic solution for thermal fixing can be obtained. On the other hand, in the second case (representing open-circuit boundary condition), due to the photovoltaic effect, photo-excited carriers will be gradually cumulated on the boundaries of the crystal to develop an open-circuit voltage under light illumination. The dc term of the space charge field, E_0, then becomes a temporal function whose time scale is close to the photorefractive time constant. Under this situation, Equations (1)~(2) become non-linear differential equations. We need to solve the temporal

growth of the dc term $E_0(t)$ first, then the space charge field (Eqs. (1~2)) can be solved by numerical methods.

For each of the two kinds of boundary conditions, two thermal fixing procedures have been practiced [10-13]: the Low-High-Low procedure (L-H-L-procedure), and the High-Low procedure (H-L procedure) or the simultaneous recording and compensating procedure (SRC procedure). Different procedures determine its particular initial conditions. In the L-H-L procedure, an electronic grating is firstly recorded by illuminating the crystal with the recording beams at Low temperature (usually at the room temperature at which proton migration is negligible). Then the crystal is heated to High temperature without light illumination so that the protons are thermally activated to form an ionic grating that neutralizes the electronic grating when. Finally an ionic grating is developed by a non-Bragg matched uniform beam at Low temperature. In the H-L procedure, the recording and compensating processes occur simultaneously by illuminating the crystal with the recording beams at High temperature, and the developing process is then carried out at Low temperature. Each phase of the above procedures produces different initial conditions for the differential equations (Eqs. (1~2)).

In summary, Equation (1)~(11) represent a general description of the temporal behavior of the thermal fixing grating. The whole thermal fixing procedure can be simulated provided appropriate boundary conditions of the crystal as well as the initial conditions of N_{D1}^{t} and n_{i1} for each phase are given. The properties of the thermal fixing can then be analyzed. Finally parameters for each recording scheme, including fixing temperature, compensation time and the recording angle for optimizing the thermal fixing efficiency can be obtained. Key results, as described by Fig.1 through Fig. 4, are summarized as following.

1. Temporal Behavior of the Space Charge Field E_{sc} in the L-H-L Procedure:

Since the strength of the photorefractive grating is proportional to the space charge field E_{sc} (via the Pockel Effect), we have shown in Fig. 1 a typical temporal behavior of the strength of E_{sc} and temperature in a L-H-L process. In the recording phase, the crystal is kept at near room temperature while illuminated simultaneously by the reference and the object waves. The space charge field increases as the electronic grating builds up. At room temperature, the conductivity of protons is much smaller than that of electrons under illumination; consequently, the proton migration is too slow to neutralize the electronic grating. When the electronic grating almost saturates at $t = t_r$, the recording beams are both cut off and the crystal is heated to a high temperature T. In this phase, the space charge field decreases as the compensating ionic grating builds up. At high temperature, the neutralizing rate due to proton migration is much faster than the thermal erasure rate of the electronic grating in the dark; consequently, the ionic grating grows until the compensation completes and then further thermal excitation cause a decrease of electronic grating. The growth of the ionic grating depends critically on the temperature T. Typically, the higher the temperature, the faster the rate. However, high temperature also causes a faster decay of the electronic grating (via thermal excitation) and tends to reduce the saturated strength of the ionic grating. There is a trade-off between the compensation time and the fixing temperature to obtain the optimum condition for maximizing the fixed diffraction efficiency. In the developing phase, the crystal is cooled to room temperature and then illuminated by a non-Bragg-matching beam at $t = t_r + t_c$. This beam causes partial redistribution of the trapped electrons (by increasing the electronic conductivity via photo-excitation), and thereby exposes the ionic grating, which manifests itself as the space charge field. Typically, the space charge field grows to a saturated value due to the redistribution of the trapped electrons and then decreases very slowly to zero due to the residual ion migration at room temperature. The decay rate determines the lifetime of the fixed grating, which can be on the order of several years for Fe-doped lithium niobate kept at room temperature. The final strength of the space-charge field (immediately after the developing processing) is determined by the compensation time and the temperature. Figure 2 shows that, the final strength of the space charge field as a function of temperature for various compensation time t_c in the range of 500 to 8000 seconds under short-circuit boundary condition. Note that for a given t_c, the value of the space charge field increases with temperature, reaches a maximum at around $T = 360 \sim 380^{\circ}\mathrm{k}$ and decreases with temperature due to the dark thermal excitation of electrons. It is also seen that the location and the magnitude of the maximum space charge field both depend on the compensation time. The maximum occurs at lower temperature provided that we take longer compensation time. Although the magnitude of the maximum value increases as the compensation time increases, the effect is relatively mild for the long compensation time. This means that, in principle, the ionic fixing can be carried out at virtually any temperature and the maximum value of the ionic grating strength increases as the fixing temperature decreases provided that a sufficiently long compensation time is allowed. In practice, however, fixing at low temperature is undesirable because it takes an unacceptably long time to reach the saturated value of the ionic grating strength at low temperature (the time constant is about 9×10^{7} seconds at room temperature). In

the example considered here, t_c=2000 seconds and $T = 373^\circ$k represent an appropriate condition, and the compensation efficiency is obtained about 82%. In addition, given a compensation time there is a temperature that produces a peak space charge field, which will result in a peak diffraction efficiency of the grating. This temperature is called the optimum compensation temperature because it gives maximum efficiency for the thermal fixing process. This figure is a useful guide for designing thermal fixing. In summary, the main factor to be considered in the optimization in the L-H-L-process is to reduce the loss during the compensation phase and to enhance the efficiency of compensation.

2. The Dependence of the Space Charge Field E_{sc} on the Compensation Temperature in the H-L Procedure:

In the H-L procedure, recording of the electronic grating and compensation of the ionic grating occur simultaneously at high temperature, and the ionic grating is developed at low temperature. Under the short-circuit boundary condition, the dependence of the final strength of the space charge field on the compensation temperature is plotted in Fig. 3 for various recording time t_c in the range of 500 to 8000 seconds. For a given short t_c (e.g. 500 seconds), the value of the space charge field increases as the compensation temperature increases from the room temperature and reaches its maximum value around $T = 390 \sim 420^\circ k$. Further increase of temperature causes the grating strength to decrease because the uniform thermal excitation tends to dominate over the photo-excitation of the interference fringes. However, for long recording time (e.g. $t_{rc} >$ 4,000 seconds), the strength of the fixed space charge field oscillates due to the large photovoltaic effect in $LiNbO_3$ crystal. In order to maximize the strength of the fixed grating, the fixing procedures (in terms of recording time and temperature) should be carefully designed. Similar to the feature observed in the L-H-L procedure, here the maximum value of the ionic grating strength also increases as the fixing temperature decreases provided that a sufficiently large t_c is allowed. There is also a trade-off between time, t_c, and temperature, T. In the example shown here (with the optimal compensation temperature $T = 413^\circ k$, and for a recording time t_c=2000 seconds), the final strength of the space charge field is about 1.6 times larger than that obtained by the L-H-L-procedure. Again, given a compensation time there is a temperature that produces a peak diffraction efficiency of the fixed grating. This figure provides useful guide for designing thermal fixing. In summary, the key for optimizing the fixing efficiency in the H-L-process is to record the electronic grating as strong as possible.

3. The Dependence of the Fixing Efficiency on the Recording Scheme:

Since the thermal fixing process depends critically on the migration of the photo-excited charge carriers and the thermally-excited protons during all phases, the recording scheme such as grating spacing (which is related to the migration length) plays a key role in thermal fixing. We have performed calculations with the fixing efficiency (defined as the multiple of the compensation efficiency and the developing efficiency) as a function of the grating spacing under short-circuit boundary condition and for L-H-L procedure. The results are shown in Figure 4. Note that the efficiency increases quickly, reaches the maximum at the recording angle around 30°, and decreases smoothly as the recording angle increases. This curve provides a useful guide for designing the recording scheme of an angle-multiplexed storage system. It is seen that the fixing efficiency is pretty flat in the range of larger recording angle. We should choose the recording angle for the angle-multiplexed holograms at around 40°.

3. OPTICAL EXPERIMENTS

To verify our calculations in the theoretical analysis section, we have performed a series of experiments with a transmission grating in highly reduced iron-doped $LiNbO_3$ crystal. The schematic diagram of the experimental setup is shown in Figure 5. A collimated argon laser beam (514 nm) was split into two ordinarily polarized beams with the intensity of 150mW/cm^2 per beam. These two beams are incident symmetrically onto the crystal with varying intersection angles. The crystal was placed in a both-end-heated oven with temperature stability of ~0.1°C. The temperature rising rate of the oven was ~0.25 °C/sec and the cooling rate is ~0.08 °C/sec. Both temperature transitions should be taken into account as the experimental results being compared with the theoretical calculations (i.e. the theoretical calculation should be modified by these transient effects).

Figure 6 shows a typical dynamic curve of the experimental result under the intersection angle of 30° outside the crystal. The diffraction efficiency is plotted as a function of time. Figure 6(a) shows that without thermal fixing, the diffraction efficiency is gradually decreased by the reading beam illumination until it is completely erased. Figure 6(b) shows that with fixing, the diffraction efficiency is revealed during the development stage. The steady state value is 4%. The diffraction efficiency of the original grating is about 13.5%. Thus, the fixing efficiency is about 30%.

The dependence of the fixing efficiency on the compensation temperature in the L-H-L procedure and under the short

circuit boundary condition are shown in Figure 7 (for varying compensation time). Notice that because of the presence of the fixing effect during temperature transition, there is still a fixed grating for zero compensation time. This fixed grating results from the temperature transition procedures. It can be seen that for a given compensation time, there is a temperature that produces a peak fixing efficiency, which will result in a peak diffraction efficiency of the fixed grating. Figure 8 shows the experimental results of the diffraction efficiency as a function of the recording temperature in H-L procedure, under short-circuit boundary condition and for the recording time of 50 mins. As expected in theoretical analysis, there is a peak of diffraction efficiency, in this case it is around $T = 120\,^{\circ}\mathrm{C}$. The trends of these curves show qualitative agreement with the above theoretic analysis.

Figure 9 show the dependence of the fixing efficiency on the recording angle for the L-H-L procedures with compensation temperature $T = 100\,^{\circ}\mathrm{C}$ and compensation time t_c=35 mins. It can be seen that, as expected in theoretical analysis, the fixing efficiency increases with the recording angle, reaches the maximum around 30°, and then decreases smoothly.

4. CONCLUSION

In summary, we have investigated the dynamic behavior of thermal fixing of photorefractive grating in $LiNbO_3$. A set of the dynamic equations have been derived and used to analyze thermal fixing under short-circuit boundary condition. Experimental results have been obtained for various conditions. Our theoretical analysis and experimental results show that two important parameters for obtaining efficient ionic grating are compensation temperature and time. The dependences of the final space charge field on temperature and compensation time have been discussed for both the L-H-L procedure and the H-L procedure. The results can be used as a useful guide for designing the thermal fixing procedures for achieving an optimal efficiency of the fixed grating.

ACKNOWLEDGEMENTS

The authors acknowledge the support of the project from National Science Council of the Republic of China under contract No. NSC88-2215-E009-008. Arthur E. T. Chiou would also like to acknowledge the support of the project under contract No. NSC88-XXXX-SXXX-XXX.

REFERENCES

[1]. J. J. Amodei and D. L. Staebler, "Holographic pattern fixing in electrooptic crystals", Appl. Phys. Lett., Vol. 18, 540-542 (1971).

[2]. D.L. Staebler, W.J. Burke, W. Philips, and J.J. Amodei, "Multiple storage and erasure of fixed holograms in Fe-doped $LiNbO_3$", Appl. Phys. Letts., Vol. 26(4), 182-184 (1975).

[3]. R. Matull and R. A. Rupp, "Microphotometric investigation of fixed holograms", J. Phys. D, 1556-1565 (1988).

[4]. P. Hertel, K. H. Ringhofer, and R. Sommerfeldt, "Theory of thermal hologram fixing and application to $LiNbO_3$:Cu", Phys. Status Solidi A 104, 855-862 (1987).

[5]. V. V. Kulikov and S. I. Stepanov, "Mechanisms of holographic recording and thermal fixing in photorefractive $LiNbO_3$:Fe", Sov. Phy. Solid State 21, 1849-1851 (1979).

[6]. A. Mendez and L. Arizmendi, "Maximum diffraction efficiency of fixed holograms in lithium niobate", Opt. Materials 10, 55-59 (1998).

[7]. A. Mehta, E. K. Chang and D. M. Smyth, "Ionic transport in LiNbO3", J. Mater. Res. 6, 851-854 (1991).

[8]. S. Orlov, D. Psaltis, and R. R. Neurgaonkar, "Dynamic electronic compensation of fixed gratings in photorefractive materials", Appl. Phys. Letts. 63, 2466-2468 (1993).

[9]. H. Vormann, G. Weber, S. Kapphan and E. Kratzig, "Hydrogen as orgin of thermal fixing in $LiNbO_3$:Fe", Solid State Comms, Vol. 40, 543-545 (1981).

[10]. B. Liu, L. Liu, and L. Xu, "Characteristics of recording and thermal fixing in lithium niobate", Appl. Opts, Vol. 37, No. 11, 2170-2176 (1998).

[11]. B. I. Sturman, M. Carrascosa, F. Agullo-Lopez, and J. Limeres, "Theoy of high-temperature photorefractive phenomena in $LiNbO_3$ crystals and applications to experiment", Phy. Rev. B, Vol. 57, No. 20, 792-805 (1990).

[12]. A. Yariv , S. Orlov, G. Rakuljic and V. Leyva, " Holographic fixing, read-out, and storage dynamics in phtorefractive

materials", Opts. Letts., Vol. 20, No. 11, 1334-1336 (1995).
[13]. M. Carrascosa, and F. Agullo-Lopez, "Theoretical modeling of the thermal fixing and developing of holographic grating in $LiNbO_3$", J. Opt. Soc. Am. B, Vol.7, No.12, 2317-2322 (1990).
[14]. N. V. Kukhtarev, V. B. Markov, S. G. Odulov, M. S. Soskin and V. L. Vinetskii, "Holographic storage in electro-optics crystals. I. Steady state", Ferroelectrics 22, 949-960 (1979).
[15]. C. Gu, J. Hong, H. Y. Li, D. Psaltis, and P. Yeh, "Dynamics of grating formation in photovoltaic media", J. Appl. Phys. 69, 1167-1172 (1991).

Symbols	Parameters	Values[13]
s	Photoionization cross section	$0.2627 cm^2 J^{-1}$
k_B	Boltzmann constant	$1.3805\times10^{-23} Jk^{-1}$
γ_R	Recombination rate	$2.5\times10^{-8} cm^3 \sec^{-1}$
D_{i0}	Diffusion constant of ion (D_e)at activation energy	$0.081 cm^2 \sec^{-1}$
ε_i	Activation energy of ion	$1.1 ev$
D_{e0}	Diffusion constant of electron (D_i) at activation energy	$0.65 cm^2 \sec^{-1}$
ε_e	Activation energy of electron	$0.2 ev$
β	Thermal ionization constant	$4\times10^{10} cm^{-3} \sec^{-1}$
ε_D	Activation energy of thermal ionization	$1 ev$
N_D	Electronic doping density	$1.89\times10^{17} cm^{-3}$
N_A	Electronic acceptor density	$6.3\times10^{16} cm^{-3}$
$n_{i,e0}$	The DC term of ionic and electronic density	$10^{19} cm^{-3}$ for ion
λ	Wavelength	$514 nm$
ε	Dielectric constant	$2.83\times10^{-10} Fm^{-1}$
P	Photovoltaic constant	$3.81\times10^{-26} cm^3 V^{-1}$
θ	Bragg angle	20°
I_0	DC term of light intensity	$150 mW cm^{-2}$
I_1	Modulation term of light intensity	$50 mW cm^{-2}$
$\mu_{e,i}$	Electronic and Ionic mobility	
K	Grating spacing	

Table 1 Definitions and values of all the parameters for theoretical analysis.

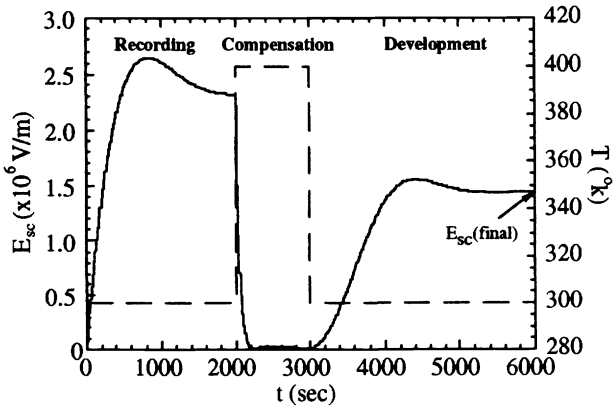

Fig. 1. Temporal dynamics of a L-H-L thermal fixing procedure.

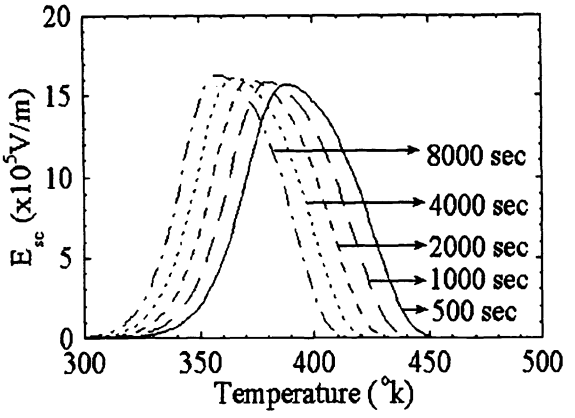

Fig. 2. Steady-state space charge field vs. compensation temperature in L-H-L procedure.

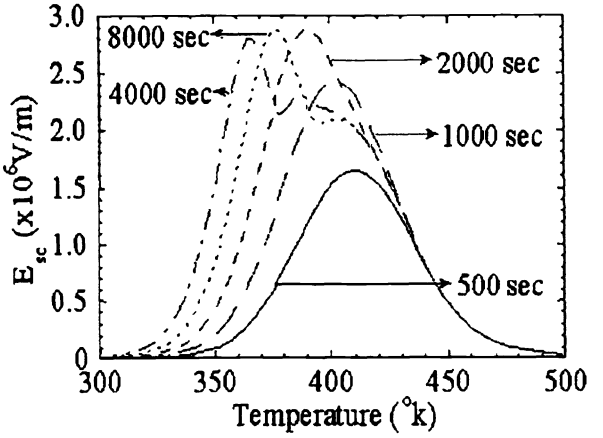

Fig. 3. Steady-state space charge field vs. recording temperature in H-L procedure.

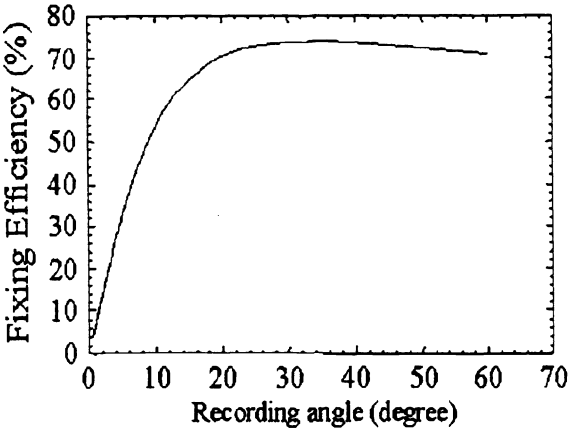

Fig. 4. Fixing efficiency vs. recording angle in L-H-L procedure.

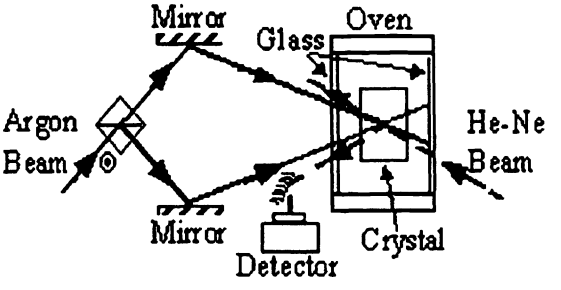

Fig.5. Scheme of the experimental setup.

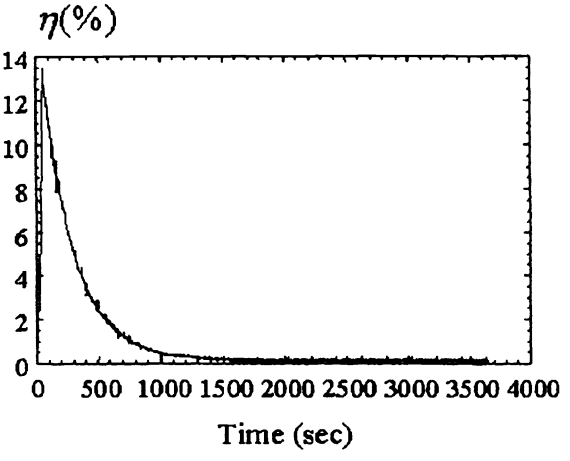

Fig.6(a). Temporal dynamics of diffraction efficiency without thermal fixing.

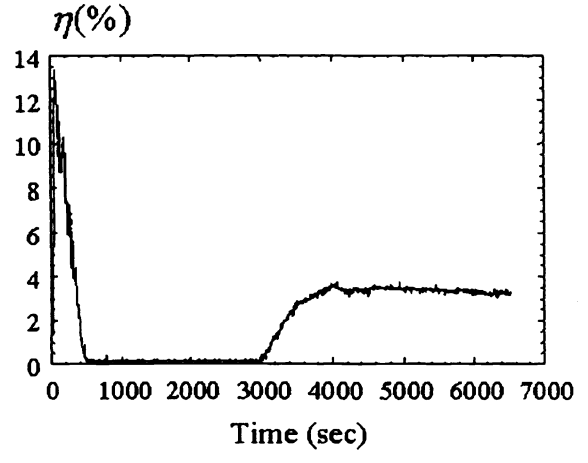

Fig.6(b). Temporal dynamics of diffraction efficiency with thermal fixing.

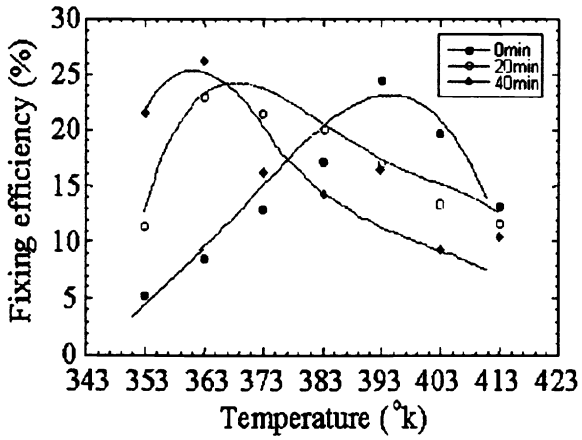

Fig.7. Fixing efficiency vs. compensa-tion temperature in L-H-L procedure (experiment).

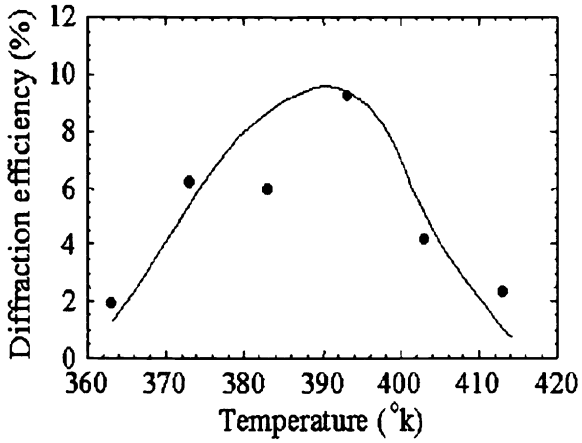

Fig.8. Fixing efficiency vs. recording temperature in H-L procedure (experiment).

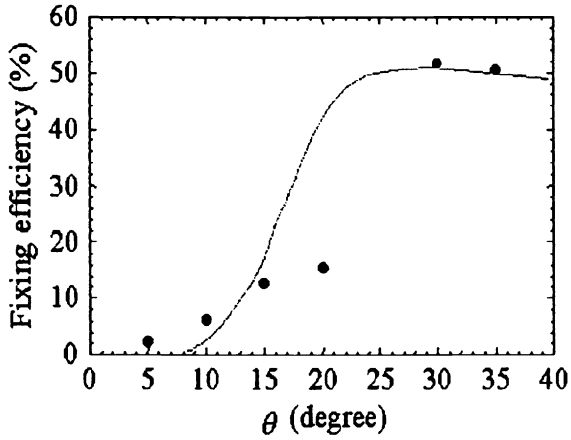

Fig. 9. Fixing efficiency vs. recording angle in L-H-L procedure (experiment).